MIPS Photometry and Spectroscopy of Protoclusters

Randolf Klein[1], Hendrik Linz[2], Jan Forbrich[3], Leslie Looney[4], Thomas Henning[2]

ABSTRACT

The onset of massive star formation and the initial conditions of the molecular cores forming massive stars are unclear. The quest is on for High-Mass Protostellar Objects (HMPOs) and the earlier High-Mass Starless Cores (HMSCs). HMPOs would be embedded in a forming cluster, a protocluster, as massive stars only form in clusters. We observed protocluster candidates with the MIPS instrument to constrain their spectral energy distribution (SED) in the far infrared (FIR). The resolution Spitzer provides is crucial to disentangle the contributions of different clumps which were resolved at other wavelengths, but not in the FIR. We will show how the Spitzer observations allowed us to improve previous luminosity estimates by e.g. finding evidence for outside heating or just resolving the FIR emission.

Subject headings: infrared: ISM, stars: formation

1. Introduction

The onset of massive star formation and its initial conditions are unclear. We need to identify objects at ever earlier stages of massive star formation. Observationally one tries to identify High-Mass Protostellar Objects (HMPOs) and the earlier High-Mass Starless Cores (HMSCs) as Beuther et al. (2007) classify the early stages. HMSCs would be found in larger Massive Starless Clumps. Once HMPOs formed, defined as accreting objects with a mass $> 8\,M_{\odot}$, the Massive Starless Clump, not starless anymore, needs to be called a

[1]Space Sciences Laboratory, University of California, Berkeley, CA 94720, USA

[2]Max-Planck-Institut für Astronomie, 69117 Heidelberg, Germany

[3]Harvard-Smithsonian Center for Astrophysics, Cambridge, MA 02138, USA

[4]Department of Astronomy, Urbana, IL 61801 USA

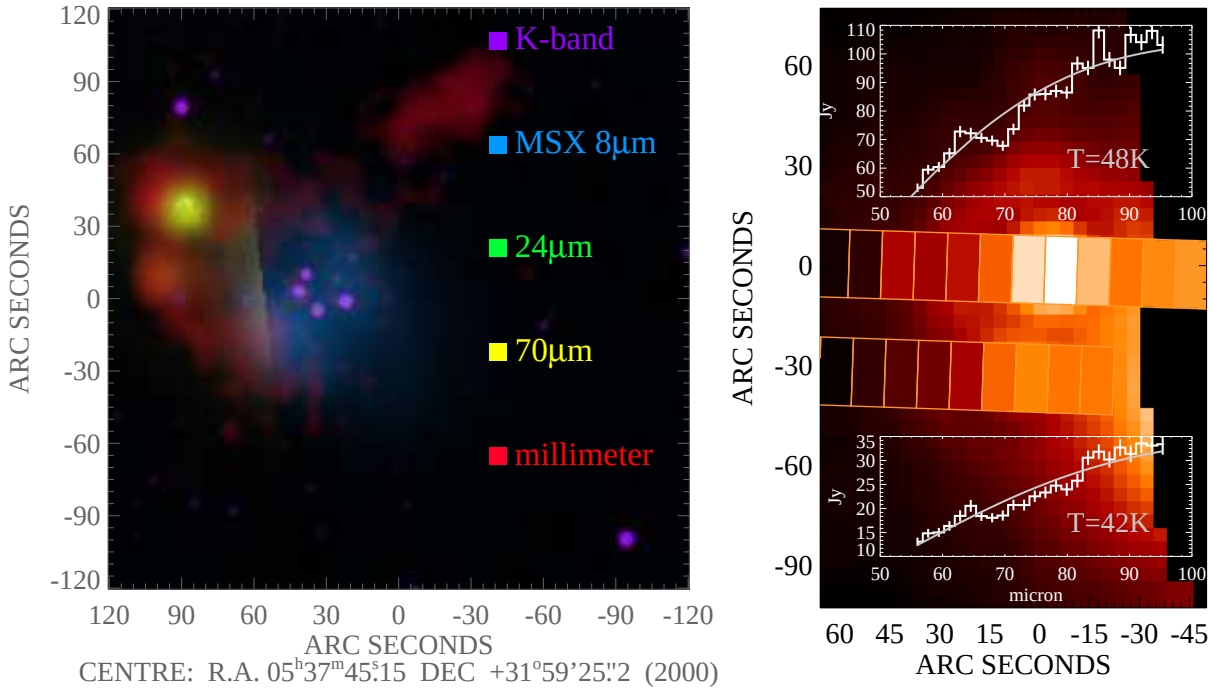

Fig. 1.— Left: NIR (2MASS) to millimeter maps of the two cores north-east of the IR-cluster IRAS 05345+3157. The MIPS observations cover only the eastern part of the area shown as the IRAS source (the IR cluster, also clearly seen in the MSX 8 μm band) would have saturated the MIPS detectors.; Right: MIPS SED observations of the two clumps. The position of the slits with the integrated intensity of the SED observation are displayed on the MIPS 70 μm map. Above and below are the obtained spectra together with a black-body fit. The error bars show 3σ as they do for all the plots of SEDs in the paper.

protocluster. As the protocluster evolves it does not contain just one HMPO but many ingredients of massive star formation like hyper-compact HII regions, hot molecular cores (HMC), outflows, masers etc. as massive stars never form alone.

Unfortunately, the evolution of these protocluster happens deeply embedded in massive cold molecular cloud clumps. The high luminosities of HMPOs get reprocessed by the envelopes. The younger they are the more deeply embedded they should be, and therefore are not detectable at short wavelengths, detectable only at far-infrared (FIR) wavelengths and longer. Thus, Spitzer observations with MIPS are important to characterize the protoclusters. Cold and massive millimeter cores are candidates for the earliest stages of massive star formation, but Spitzer with its unprecedented sensitivity and spatial resolution allows to constrain the SEDs of individual clumps, which is crucial to for a correct characterization.

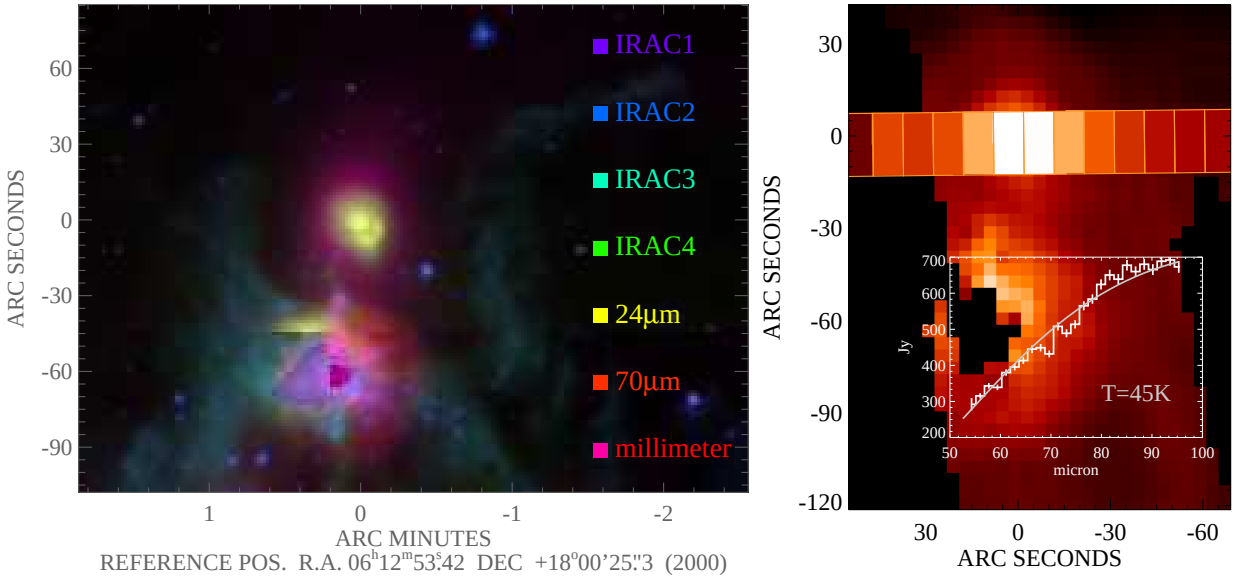

Fig. 2.— S255IR and S255N from the MIR to the millimeter; Right: The MIPS SED observation. The position of the slit with the integrated intensity is displayed on the MIPS 70 μm map. The SED follows a black-body spectrum with a temperature of 45 K.

2. Observations

We carefully selected good candidate molecular clumps for being in an early stage of intermediate-mass or massive star formation. Here, we present three targets selected from our (sub-)millimeter survey targeting bright IRAS sources (Klein et al. 2005) and one target selected from sub-millimeter follow-up observations of Infra-Red Dark Clouds (IRDCs) detected by the MSX satellite (Nyman et al. 2001). The common thread to all of these sources is that they do not show any near- or mid-infrared emission, and with one exception, no cm radio emission. Another important selection criterion was that the targets are well separated from bright FIR sources as not to saturated the MIPS detector.

3. Results

3.1. IRAS 05345+3157 (1.8 kpc)

Two candidate clumps have been detected by their 870 μm emission 1′ north-east of IRAS 05345+3157 (Fig. 1). The cores have gas masses of around 50 $M_\odot$ and 40 $M_\odot$ and could host protoclusters of intermediate mass (Klein et al. 2005). Towards the IRAS source, a cluster has already formed. It has burned a cavity in its parental cloud leaving a ring of dust

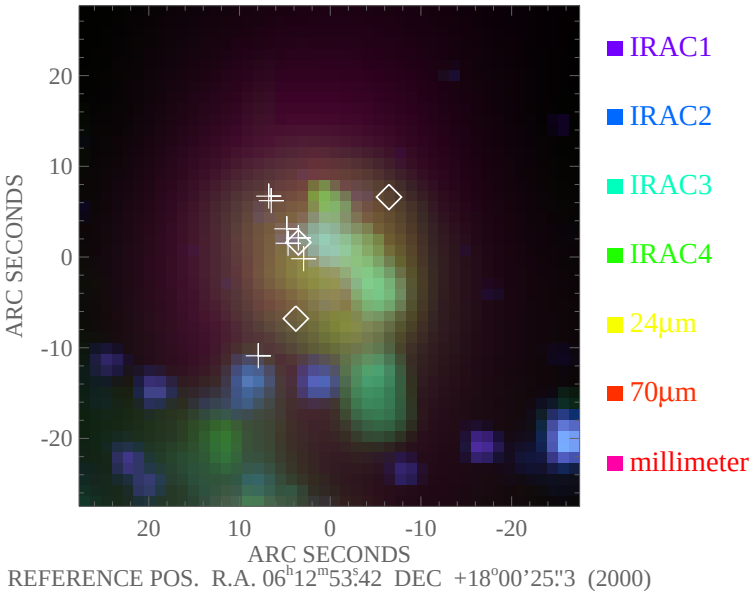

Fig. 3.— Zoom in on S255N: diamonds mark positions of SMA1 to 3 (Cyganowski et al. 2007), crosses mark methanol masers (Kurtz et al. 2004)

and gas with the two prominent clumps. Our Spitzer observations allow to analyze the FIR emission of the two clumps separately. The northern, more massive clump is twice as bright as the southern clump. Assuming a distance of 1.8 kpc the clumps emit about 400 $L_\odot$ and 200 $L_\odot$, respectively. Fitting a blackbody to the MIPS spectra yields a temperatures around 45 K for both cores. Taking into account the lack of MIR and NIR emission from these cores, we conclude that there are intermediate-mass protostars embedded in these clumps. Given that the MIPS SEDs of the two cores are very similar (expressed by the same temperature of the blackbody fit), the two clumps are in a similar evolutionary stage containing deeply embedded protostars.

3.2. S255 N (2.5 kpc)

S255IR (IRAS 06099+1800) is a very young infrared cluster hosting massive B stars and massive young stellar objects in different evolutionary stages (Howard et al. 1997; Itoh et al. 2001). North of it is the even younger clump S255N. S255N is located at the northern end of a cloud ridge between the two large HII regions S255 and S257. Kurtz et al. (1994) have detected an ultra-compact HII (UCHII) region in S255N. Cyganowski et al. (2007) resolved the cloud clump S255N into 3 cores: SMA1 to 3 (Fig. 3). SMA2 and 3 do not show further signs of star formation. The dominant core SMA1 is located where a line of methanol masers (crosses in Fig. 3) starts. It extends opposite to the cometary UCHII region (Kurtz et al. 1994). Weak emission from shocked H_2 gas, only present in the IRAC2 band (4.5 μm), also indicates the presence of a jet. In the other IRAC bands, the UCHII region is traced to the

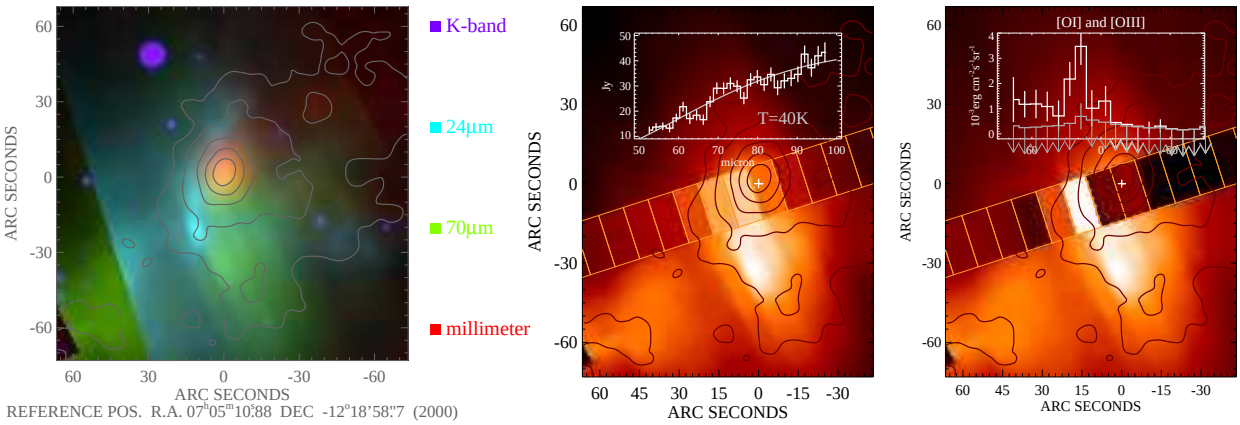

Fig. 4.— Left: UYSO 1 from the NIR (2MASS) to the millimeter. Contours are the JCMT 850 μm map; Middle: The location of slit for the MIPS SED observation and the integrated intensity is plotted on top of the MIPS 70 μm map. The inset shows the background subtracted spectrum of UYSO 1 and blackbody fit to it; Right: Same as in the middle but the slit shows the [OI] intensity peaking 20″ east of the core and so does the inset which additionally shows the marginal detection of the [OIII] line.

south-west. Our MIPS observations resolve S225N for the first time in the FIR. We derived a luminosity of almost $10^4\,L_\odot$ which is exactly the luminosity Kurtz et al. (2004) derived from the UCHII region inferring a B0.5 star. Clearly, this is a very young massive star-forming region, but past its protostellar phase as an UCHII region has already developed.

3.3. UYSO 1 (1.0 kpc)

After its detection in the millimeter continuum (Klein et al. 2005), the cold core in the region of IRAS 07029-1215, UYSO 1, has been investigated in detail by Forbrich et al. (2004). A very young ($< 1.5 \cdot 10^4$ yr) but powerful and massive ($5.4\,M_\odot$) outflow was detected. The non-detection in the NIR and MIR further indicated a very early evolutionary state. Even our Spitzer observations with MIPS did not reveal any point source in UYSO 1 (Fig. 4). However, we detect extended FIR emission for the cloud core. The core seems to be irradiated from the east – from the cluster IRAS 07029-1215. The 24 μm map shows a sharp emission ridge at the eastern edge of the core. Also the 70 μm emission can be described as a bar east of the core center extending in north-south direction. Furthermore, the MIPS SED observations detected the [OI] and [OIII] lines at 63 and 88 μm, respectively. They also peak sharply at the eastern cloud edge (Fig 4). Apparently the radiation hitting the cloud there is radiated away in these important cooling lines.

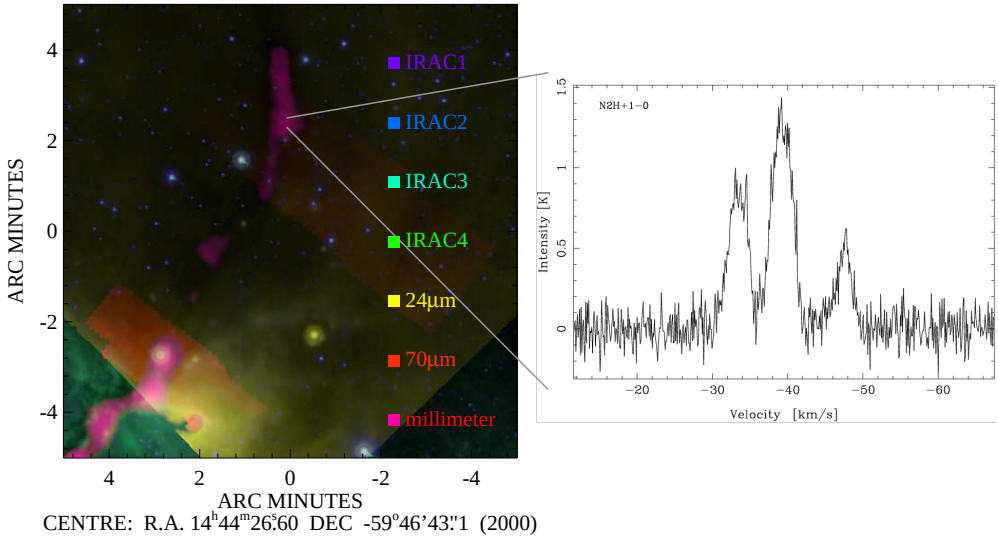

Fig. 5.— Left: IRDC 316.71+0.082 from the MIR to the millimeter. The millimeter emission from the filamentary IRDC is clearly detected. However the filament in the north-west does not appear in emission at any shorter wavelength. Note that especially the MIPS 70 μm does not cover the whole region. Right: N_2H^+ 1-0 transition observed in the clump in the north-western filament with surprising line widths.

In order to estimate the luminosity intrinsic to the objects embedded UYSO 1, we subtracted the extended emission caused by the outside heating. After the subtraction of the extended emission, aperture photometry resulted in a flux density of <27 mJy and 31 Jy at 24 and 70 μm, respectively. That translates to a luminosity of only $\sim 100\,L_\odot$ intrinsic to the sources embedded in the core which should be driving the detected massive outflows. A paper trying to resolve this puzzle is in preparation (Forbrich et al. 2008).

3.4. IRDC 316.71+0.082 (2.9 kpc)

Infra-red dark clouds (IRDCs) are in the discussion for hosting high-mass protostars, as they present very dense environments causing extinction down to 8 μm. IRDC 316.71+0.082 is an example for such an IRDC identified in MSX data, and then observed by us with MIPS, by GLIMPSE with IRAC, and by us with SIMBAD in the mm-continuum (Fig. 5). At the south-east end of the filamentary cloud, a cluster has already formed, but the rest of the filament is still dark in the NIR and MIR. Despite a high mass of about 500 $M_\odot$, no indications of on-going star formation is detected, yet. MIPS sees extinction even at 24 μm and a marginal detection at 70 μm whereas other IRDCs show 70 μm flux densities of the order of 10 Jy (Linz et al. 2007; Hennemann et al. 2007). Molecular line widths are broader

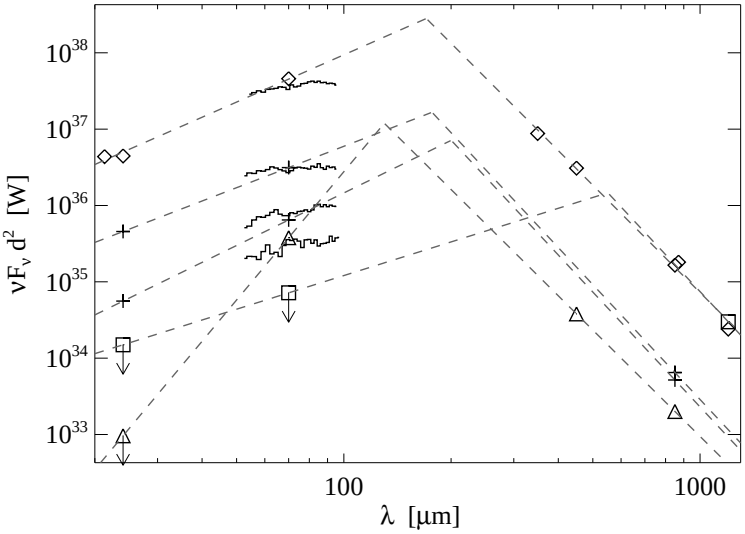

Fig. 6.— Comparing SEDs of the five cores from MIPS observations and (sub-)mm photometry: Diamonds – S255N, Crosses – Both cores near IRAS 05345+3157, Triangles – UYSO 1, Squares – IRDC 316.71+0.082; The SEDs are displayed as $\nu F_\nu d^2$ where d is the distance to compare the cores despite their different distances. The dashed lines connect the data points for each core. See Sect. 4 for further discussion.

than expected for low-mass cores (N_2H^+ 1-0 spectrum in Fig. 5). Has turbulent support of the clump prevented it from collapsing? These are all very good indications that this is really a high-mass starless core! Interferometric observations are underway to investigate this IRDC further.

4. Summary

The four presented clumps or cores have in common that they are prominent millimeter continuum sources but have no appreciable NIR or MIR emission associated with them. The masses range from 30 $M_\odot$ (UYSO 1) up to 500 $M_\odot$ (IRDC 316.71+0.082) while the distances vary from 1.0 to 2.9 kpc. Figure 6 compares the SEDs of all discussed five cores. The dashed lines connect the MIPS observations on the short wavelength side and the (sub-)millimeter observations on the other side. They also indicate the spectral indexes on both sides of the maximum of the SED. Where we had only one sub-mm point a spectral index of -5 was assumed for νF_ν i.e. a dust emissivity exponent of $\beta = 2$, similar to the cores where more data are available.

The two cores near IRAS 05345+3157 and S255N display similar SEDs peaking around 200 μm despite their different masses and luminosities. The common trait is a deeply embedded object. The internal heating gives rise to the MIR emission, but the envelope is massive enough to contain cold dust responsible for the large FIR & sub-mm luminosity. Given that a lot of material is available, it is likely that accreting protostars are embedded, except that at least one massive protostar in S255N has already reverted the accretion flow and developed an UCHII region.

Much different is the massive clump, IRDC 316.71 + 0.082 with $500\,M_\odot$. It is hardly detected by our MIPS observations while S255N with a mass in the same order of magnitude, ($220\,M_\odot$, Minier et al. 2005) is with $10^4\,L_\odot$ the most luminous clump. The lack of MIR emission could be explained by the lack of internal heating making IRDC 316.71 + 0.082 a very good candidate for a massive starless clump where the initial properties of massive star-forming cores can be studied.

Another oddball in this set is UYSO 1 mainly because we see evidence for external heating. This makes it difficult to reliably determine the luminosity of the sources embedded in UYSO 1, but it seems to be of the order of only $100\,L_\odot$. However, the detected massive outflow cannot be easily explained with a $100\,L_\odot$ protostar. Also the lack of MIR emission indicating an extremely young object will be discussed by Forbrich et al. (2008). *Stay tuned.*

This work is based on observations made with the *Spitzer Space Telescope*, which is operated by the Jet Propulsion Laboratory (JPL), California Institute of Technology under NASA contract 1407.

REFERENCES

Beuther, H., Churchwell, E. B., McKee, C. F., & Tan, J. C. 2007, in Protostars and Planets V, ed. B. Reipurth, D. Jewitt, & K. Keil, 165–180

Cyganowski, C. J., Brogan, C. L., & Hunter, T. R. 2007, AJ, 134, 346

Forbrich, J., Klein, R., Stanke, T., et al. 2008, in preparation

Forbrich, J., Schreyer, K., Posselt, B., Klein, R., & Henning, T. 2004, ApJ, 602, 843

Hennemann, M., Birkmann, S. M., Krause, O., & Lemke, D. 2007, in IAU Symposium, Vol. 237, IAU Symposium, ed. B. G. Elmegreen & J. Palous, 424–424

Howard, E. M., Pipher, J. L., & Forrest, W. J. 1997, ApJ, 481, 327

Itoh, Y., Tamura, M., Suto, H., Hayashi, S. S., Murakawa, K., Oasa, Y., Nakajima, Y., Kaifu, N., Kosugi, G., Usuda, T., & Doi, Y. 2001, PASJ, 53, 495

Klein, R., Posselt, B., Schreyer, K., Forbrich, J., & Henning, T. 2005, ApJS, 161, 361

Kurtz, S., Churchwell, E., & Wood, D. O. S. 1994, ApJS, 91, 659

Kurtz, S., Hofner, P., & Álvarez, C. V. 2004, ApJS, 155, 149

Linz, H., Klein, R., Looney, L., Henning, T., Stecklum, B., & Nyman, L.-Å. 2007, in IAU Symposium, Vol. 237, IAU Symposium, ed. B. G. Elmegreen & J. Palous, 440–440

Minier, V., Burton, M. G., Hill, T., Pestalozzi, M. R., Purcell, C. R., Garay, G., Walsh, A. J., & Longmore, S. 2005, A&A, 429, 945

Nyman, L.-Å., Lerner, M., Nielbock, M., Anciaux, M., Brooks, K., Chini, R., Albrecht, M., Lemke, R., Kreysa, E., Zylka, R., Johansson, L. E. B., Bronfman, L., Kontinen, S., Linz, H., & Stecklum, B. 2001, The Messenger, 106, 40